Applied Physics Letters

Single pixel camera methodologies for spatially resolved acoustic spectroscopy

Cite as: Appl. Phys. Lett. **118**, 051102 (2021); https://doi.org/10.1063/5.0040123
Submitted: 11 December 2020 . Accepted: 21 January 2021 . Published Online: 02 February 2021

Rikesh Patel, Steve D. Sharples, Matt Clark, Mike G. Somekh, and Wenqi Li

Applied Physics Letters ARTICLE scitation.org/journal/apl

Single pixel camera methodologies for spatially resolved acoustic spectroscopy

Cite as: Appl. Phys. Lett. **118**, 051102 (2021); doi: 10.1063/5.0040123
Submitted: 11 December 2020 · Accepted: 21 January 2021 ·
Published Online: 2 February 2021

Rikesh Patel,[1,a)] Steve D. Sharples,[1] Matt Clark,[1] Mike G. Somekh,[1,2] and Wenqi Li[1]

AFFILIATIONS

[1]Optics and Photonics Group, Faculty of Engineering, University of Nottingham, University Park, Nottingham NG7 2RD, United Kingdom
[2]Nanophotonics Research Center, Shenzhen University, Shenzhen 518060, China

[a)]Author to whom correspondence should be addressed: rikesh.patel@nottingham.ac.uk

ABSTRACT

Spatially resolved acoustic spectroscopy (SRAS) is a laser ultrasound technique used to determine the crystallographic orientation (i.e., microstructure) of materials through the generation and measurement of surface acoustic wave velocity on a sample. Previous implementations have used a grating pattern imaged onto the surface to control the frequency of the generated wave in a single direction—grain orientation can be computed by acquiring wave velocities in different directions on the surface (gathered by physically rotating the grating pattern). This paper reports an advance to this methodology, inspired by single pixel cameras, using a coded grating pattern, created using a spatial light modulator, to excite surface acoustic waves in multiple directions simultaneously. This change to the optical arrangement can simplify the overall system alignment, remove mechanical complexities, and is well suited for point-by-point full orientation imaging, potentially allowing for faster orientation imaging using SRAS microscopy. Improvements to the robustness of measurement may be expected to extend the applicability of SRAS in the materials science field. To demonstrate this methodology, experiments were conducted on isotropic and anisotropic samples.

Spatially resolved acoustic spectroscopy (SRAS) is a nondestructive laser ultrasound technique capable of rapidly mapping the velocities of generated surface acoustic waves (SAWs) on the surface of materials.[1,2] In a typical configuration, a binary grating pattern with fixed fringe separation, λ, is imaged onto a surface using a short pulsed laser, forcing thermo-elastic generation of SAWs along one predominant axis. Since the wavelength of the SAWs is fixed by λ, the frequency of the generated wave is proportional to the phase velocity along the particular direction, where $v = f \times \lambda$.[1] A separate continuous wave laser is used to measure the perturbation on the sample surface, illustrated in the upper part of Fig. 1. When the material under inspection can be approximated as an infinite half-space (practically satisfied if the thickness of the sample is much larger than λ), then the generated wave is a non-dispersive Rayleigh wave; for thinner samples, the waves generated are predominantly Lamb waves.[3] The spatial resolution of the system is determined by the total area of the generation pattern incident on the sample surface, which is practically determined by λ, the number of fringes in the pattern, generation laser pulse energy, and the required signal amplitude.[2]

In order to determine the crystallographic orientation at different points on the surface of a sample, the SAW velocity is required over a range of rotational angles on the 2D surface [i.e., the velocity as a function of propagation direction on the sample surface, $v(x, y, \theta)$]. The measured velocity surfaces are compared to velocities calculated using elastic constant and density information of different materials from the literature—since these velocity surfaces vary with orientation, the local texture can be obtained by the best fit between the measured and calculated velocity surfaces corresponding to different orientations. This approach has been used to map the material microstructure of aluminum, steel, nickel alloys,[4] and titanium alloys.[1,2,5,6] Through coating or adjustment of the generation and detection laser wavelength, it is also possible to image other materials such as silicon solar cells.[7] For SRAS, a measurement corresponds to the velocity of a surface wave mode that has the largest out-of-plane amplitude under the generation area — obtaining all required SAW velocities for a single mapped point requires making measurements while rotating the grating pattern along with the point of detection. This is currently done mechanically and is an inspection speed bottleneck in the system.

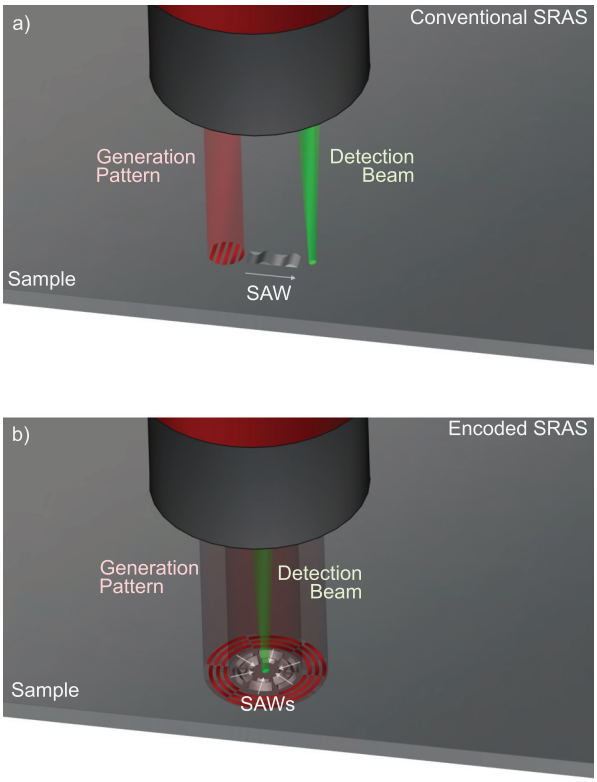

FIG. 1. Schematic of the (a) conventional SRAS system and (b) encoded SRAS system. In both cases, a pattern is imaged onto a sample using a pulsed IR laser (as describe in previous publications[1,2])—SAWs are generated which are detected using a green continuous-wave laser. A vibrometer employing a heterodyne interferometry is used to measure the waveform of the surface perturbation produced by the generation laser. To determine the material property, the SAW must be measured in multiple directions—conventional SRAS requires the pattern and detection beam to rotate through at least 180°, while the encoded SRAS system only requires a change in pattern.

The idea behind the single pixel camera (SPC) is that a number of linear projections of a signal or image can be used for reliable reconstruction—the number of projections required depends on the information content of the signal.[8] Light from a scene can be encoded using a changing pseudo-random 2D binary pattern, e.g., on a digital mirror device, with the encoded scene detected entirely on a single light detector.[9] With knowledge of the patterns and the measured light intensities corresponding to each sequence, images can be reconstructed. If the image is sparse in some domain, it to possible to make fewer measurements than the number of pixels in the recovered image.[10,11] In the present work, however, we do not apply sparsity other than to recognize that waves traveling along the same line in opposite directions will have the same velocity.

This paper explores the use of coded segmented patterns to generation surface acoustic waves for the SRAS system, as shown in Fig. 1(b). If a generation pattern is produced such that the surface waves will always travel to a single point (i.e., the center of a pattern), then the overall optical design can be simplified, with mechanical rotation complexities removed, and improving data acquisition times for full orientation imaging.

In a conventional SPC, the image to be reconstructed is illuminated by a sequence of patterns, with each pattern in the sequence integrated onto a single detector. Since the illumination patterns in the sequence, as well as the detector output at each position in the sequence are known, the image may be reconstructed, or in other words, the different image points can be isolated from each other. In the case of SRAS, the "image points" correspond to the segments associated with different propagation directions—it is then natural for the detector to be located at the center of these segments where the summation takes place. The vibrometer at the center thus fulfills the role of a single pixel detector. It is critical that the segments are illuminated with a unique code so that, after applying the sequence of codes, the wave pattern from each segment may be separated.

With these considerations, a SAW generation pattern consisting of concentric arcs, with the detection point in the center of the pattern, was used. Radially, this forms an intensity grating pattern on the sample with each segment consisting of light and dark arcs (see Fig. 2)—this provides wave focusing at the detection point thus maximizing the displacement at the detection point. The radial grating pattern was segmented, and each opposing segment pair was encoded using a known pseudo-random code. Since opposing segments contain the same velocity information, the 32 segment array has only 16 independent values. Indeed, mirroring the pattern at 180°, allows the signals from the opposite sectors to interfere constructively to create a larger detectable amplitude. Each sector generates a surface wave that propagates along the radial axis toward the center of the arcs, where the single point detector point is located. Figure 2 shows an example generation pattern with 32 segments (16 segment pairs), produced using Hadamard coding. We will take segment "c" to illustrate the idea, this is illuminated with [−1 −1 1 1 −1 −1 1 1 −1 −1 1 1 −1 −1 1 1] as shown by the light and dark blocks in the c column of the coding diagram of Fig. 2. Physically, the code values are obtained by switching the phase of the grating (swapping the light and dark sections) so that 1 corresponds to a grating phase of 90° and −1 to −90°. This inverts the temporal phase of the SAW that is generated by that segment.

The detection process may be summarized as follows: (1) apply the fixed period grating structure with the appropriate phase corresponding to the Hadamard code element for each segment pair. (2) For each element in the Hadamard code, acquire the corresponding temporal waveform. In the present case, 16 waveforms are acquired, corresponding to the elements in the Hadamard code. The waveforms at this stage are a summation of the outputs from each segment pair. (3) Since the codes associated with each segment pair are orthogonal, the waveforms associated with each segment pair are obtained by multiplying the waveforms by the code associated with the desired segment pair. This selects out the specific segment pair and this process is repeated for each segment. The orthogonality suppresses signals from other segments and reinforces the signal from the desired segment. (4) Take the recovered waveform from each segment pair and Fourier transform to acquire the predominant frequency and convert to a velocity by multiplying by the grating period.

This process may be formalized as follows: the reconstructed signal for the i^{th} segment pair is given by $R_i(t) = M(t) \times H_i$, where $R_i(t)$ is the reconstructed signal corresponding to the ith segment pair, M is the measured signal at the point detector, and H_i is Hadamard code associated with the ith segment pair. This method of

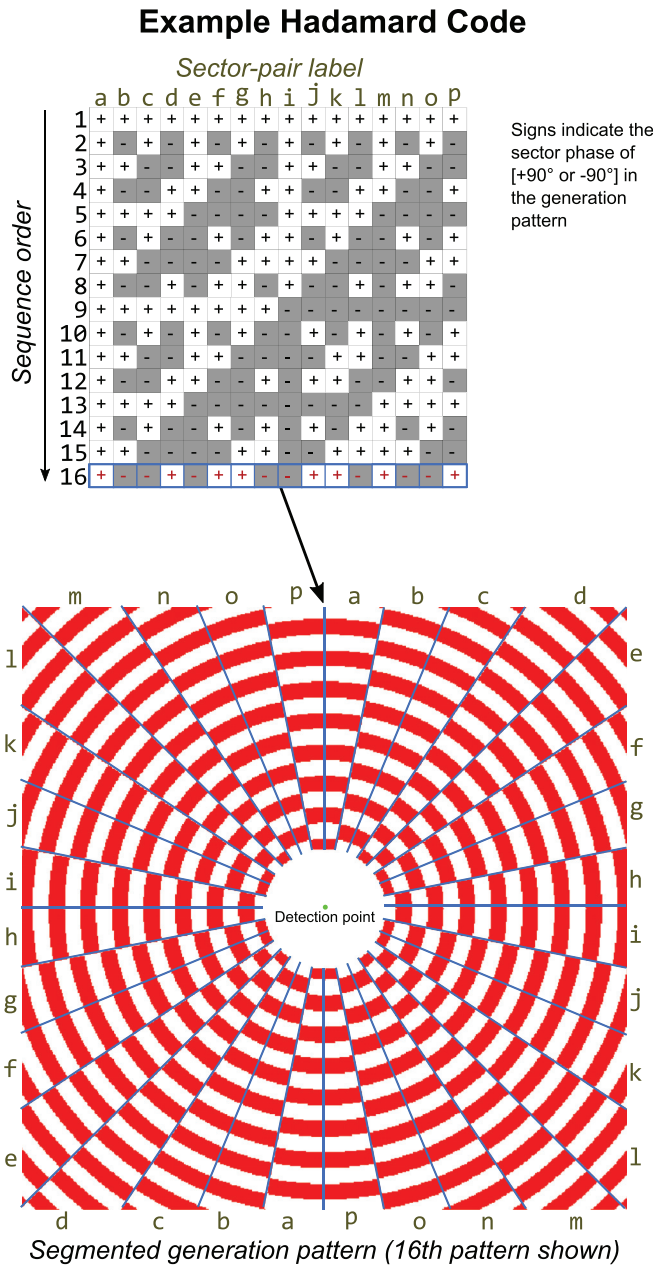

FIG. 2. Table of Hadamard codes (top) used to encode a 32 segment radial SRAS pattern (bottom). The codes are displayed on the SLM sequentially and are measured for each code. The green point indicates the centrally located detection point. This particular pattern represents the 16th code in the sequence.

reconstruction is similar to that used in the fields of ultrasound array testing[12] and structured light systems.[13]

It is worth pointing out that a truly orthogonal code such as a Hadamard code requires both positive and negative values. In ultrasonics where we have access to the waveform associated with the acoustic field, this may be easily implemented by inverting the phase of the signal. In optics where only intensity measurements are usually available, it is necessary to subtract a background image to replicate a bipolar output, there is thus a distinct advantage of applying this coding methodology in ultrasonics.

The new system was rearranged with the SAW generation pattern constructed using a 512×512 element spatial light modulator (SLM; Boulder Nonlinear Systems DS XY1110), which can support frame rates of up to 1 kHz. A high sensitivity vibrometer (Polytec OFV-5000) was used to detect the surface perturbation at the center of the generation pattern. It may be shown that, in principle, the signal to noise ratio (SNR) of the present approach is similar to a conventional SRAS with the same incident light energy.

Initial tests using the encoded pattern SRAS system were implemented on a glass substrate coated with a thin layer of aluminum (1–2 μm) in order to improve surface wave generation and detection. As glass is an amorphous solid, Rayleigh waves propagate at a constant speed in all directions, and as such is often used for calibration.

It is possible to use the SLM to illuminate a pair of opposing sectors i.e., without employing sector encoding. Figure 3 shows measurements made using the vibrometer when a single sector pair was illuminated (top) and when a complete encoded pattern was illuminated (bottom) on the glass sample using the SLM. The pattern used had 32 total sectors (16 sector pairs) shown on the left of the figure, with the pattern wavelength, $\lambda = 200\,\mu$m. The upper right side of the figure shows the measured signal arising from the pair of gratings shown in the left. The lower right figure shows the waveform after the reconstruction algorithm was applied to the coded pattern. It should be noted that in this implementation, using the SLM to illuminate a single sector pair means that only a fraction of the laser energy translates to wave generation when compared to illuminating a full pattern. Additionally, there is strong common-mode noise (caused by the generation laser) visible in the single sector pair waveform which is significantly reduced in the encoded waveform after the reconstruction algorithm is applied.

In order to verify the multi-direction SAW velocities obtained after applying the reconstruction algorithm, the results from different samples were compared against results obtained using a conventional SRAS system. Figure 4 shows the radial SAW velocity spectra—polar plots that show the velocity spectrum in all directions on a sample surface—conducted on glass (top) and single crystal nickel samples (bottom), made using the encoded pattern SRAS system (left) and conventional SRAS system (right). For these results, 16 sector pairs were used. To evaluate whether the results match, the shape of the radial velocity spectra map should be compared.

The glass sample shows constant velocity with respect to the propagation direction (to within experimental error) for both SRAS implementations, consistent with the isotropic nature of the material. The standard deviation in the SAW velocity was 16 ms^{-1} and 11 ms^{-1} for the encoded and conventional SRAS systems, respectively. Nickel was chosen as the other measurement sample as it is highly anisotropic—both measurements show a similar shape demonstrating the encoded pattern SRAS system feasibility. Since this sample is anisotropic, the standard deviation is not indicative of the noise. It is apparent, however, that the signal to noise in the anisotropic sample is not as good as the isotropic sample, this is because the light absorption and the thermoelastic ultrasonic generation efficiency are not so good in nickel. This effect arises from the material rather than any specific measurement methodology.

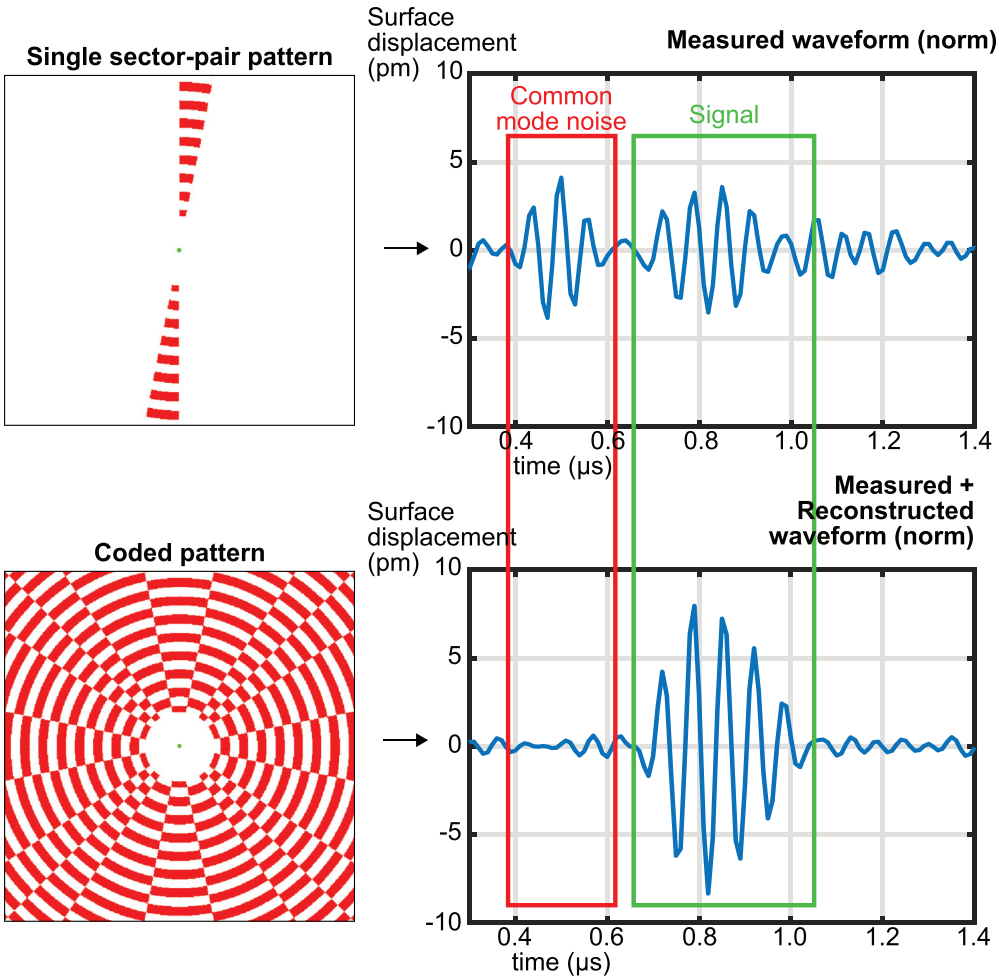

FIG. 3. Waveforms of measured/reconstructed signals (right) give the pattern imaged on an aluminum coated glass substrate (left). The single sector pair signal shows common-mode noise (measured using a commercial vibrometer with a conversion of 1 V/50 nm with capture triggered by the measurement of the generation laser pulse)—this is suppressed in the encoded reconstructed measurement signal.

It is important to understand how the present encoding approach can dramatically improve the usability of orientation measurement using SRAS.[14] For a single image, revealing the grain structure in a qualitative manner propagation in a single direction often suffices, but quantification of orientation requires velocity measurements at typically 10 different propagation directions. There are two ways that this is done currently: (i) rotate the sample, rescan, and then reregister the images. This requires a raster scan for each propagation direction greatly slowing the data acquisition process. Rotation of the sample can also be practically inconvenient for large components, or (ii) rotate the optics so the grating and detection direction are changed, this usually requires realignment of the optics, as well as reregistration of the images. This also requires multiple raster scans that drastically increases data acquisition time. The modest increase in complexity in the signal generation and processing thus greatly reduces the mechanical inconvenience and complexity of quantitative SRAS.

In conclusion, this paper has presented a new implementation of the SRAS system in which the method of generating multiple and separable SAWs propagating in different directions has been achieved using a coding methodology analogous to the SPC. This enables full multi-direction scans by sending generation patterns to an SLM, where sectors within the pattern are excited with different orthogonal codes. As shown in Fig. 4, the results from both isotropic and anisotropic samples show that the acquired multi-direction velocities with the new method are comparable to those obtained with the conventional SRAS system.

This methodology has the potential to remove mechanical translation complexities, is well suited for point-by-point full orientation mapping, and can improve system robustness through a simplification of the system arrangement. Optical alignment of the system remains important as velocity error is dependent on the detection point position relative to the center of the generation pattern—this may be overcome using additional optical methods (e.g., using beam-steering and

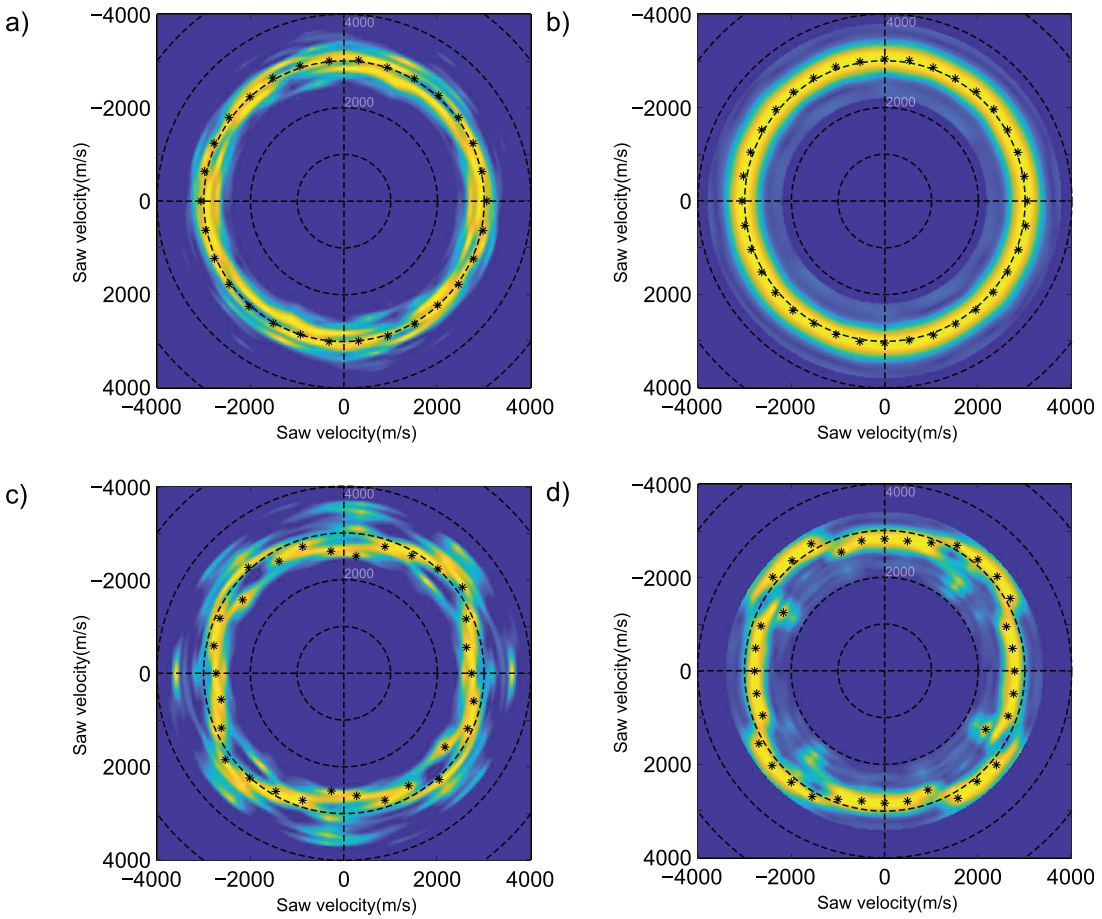

FIG. 4. Measured radial velocity spectra maps of aluminum coated glass [(a) and (b)] and single crystal nickel samples [(c) and (d)]. The left figures [(a) and (c)] were produced using the encoded pattern SRAS system and the right figures [(b) and (d)] were produced using the conventional SRAS system to allow comparison. Asterisks indicate maximum response after Gaussian fitting, yellow indicates high response, and blue indicates low response.

reticles) for alignment. Additionally, the system requires the pattern to be correctly focused to maximize the measured signal.

In contrast to many optical systems, the Hadamard code in this method is implemented with out-of-phase segments giving true +1 and −1 codes without a DC component—the lack of DC component helps suppress common-mode noise and to enhance the detectability of small signals.

AUTHORS' CONTRIBUTIONS

All authors contributed equally to this work.

This work was supported by the Engineering and Physical Sciences Research Council (Grant Nos. EP/L022125/1 and EP/G061661/1) through the "UK Research Centre in Nondestructive Evaluation" and "Advanced Ultrasonics Platform" and Shenzhen Science and Technology Innovation Commission (No. KQTD20180412181324255).

DATA AVAILABILITY

The data that support the findings of this study are available from the corresponding author upon reasonable request.

REFERENCES

[1]W. Li, S. D. Sharples, R. J. Smith, M. Clark, and M. G. Somekh, "Determination of crystallographic orientation of large grain metals with surface acoustic waves," J. Acoust. Soc. Am. **132**, 738–745 (2012).
[2]R. J. Smith, W. Li, J. Coulson, M. Clark, M. G. Somekh, and S. D. Sharples, "Spatially resolved acoustic spectroscopy for rapid imaging of material microstructure and grain orientation," Meas. Sci. Technol. **25**, 055902 (2014).
[3]I. A. Viktorov, *Rayleigh and Lamb Waves: Physical Theory and Applications*, Ultrasonic Technology (Plenum Press, 1970).
[4]A. Mark, W. Li, S. Sharples, and P. Withers, "Comparison of grain to grain orientation and stiffness mapping by spatially resolved acoustic spectroscopy and ebsd," J. Microsc. **267**, 89–97 (2017).
[5]L. W. Koester, H. Taheri, T. A. Bigelow, P. C. Collins, and L. J. Bond, "Nondestructive testing for metal parts fabricated using powder-based additive manufacturing," Mater. Eval. **76**, 514–524 (2018).
[6]P. Dryburgh, R. J. Smith, P. Marrow, S. J. Lainé, S. D. Sharples, M. Clark, and W. Li, "Determining the crystallographic orientation of hexagonal crystal structure materials with surface acoustic wave velocity measurements," Ultrasonics **108**, 106171 (2020).
[7]R. Patel, W. Li, R. J. Smith, S. D. Sharples, and M. Clark, "Orientation imaging of macro-sized polysilicon grains on wafers using spatially resolved acoustic spectroscopy," Scr. Mater. **140**, 67–70 (2017).

[8]E. J. Candès, J. K. Romberg, and T. Tao, "Stable signal recovery from incomplete and inaccurate measurements," Comm. Pure Appl. Math. **59**, 1207–1223 (2006).
[9]M. P. Edgar, G. M. Gibson, and M. J. Padgett, "Principles and prospects for single-pixel imaging," Nat. Photonics **13**, 13–20 (2019).
[10]M. F. Duarte, M. A. Davenport, D. Takhar, J. N. Laska, T. Sun, K. F. Kelly, and R. G. Baraniuk, "Single-pixel imaging via compressive sampling," IEEE Signal Process. Mag. **25**, 83–91 (2008).
[11]N. Huynh, F. Lucka, E. Zhang, M. Betcke, S. R. Arridge, P. C. Beard, and B. T. Cox, "Single-pixel camera photoacoustic tomography," J. Biomed. Opt. **24**, 1 (2019).
[12]B. W. Drinkwater and P. D. Wilcox, "Ultrasonic arrays for non-destructive evaluation: A review," NDT E Int. **39**, 525–541 (2006).
[13]T. Bell, B. Li, and S. Zhang, "Structured light techniques and applications," in *Wiley Encyclopedia of Electrical and Electronics Engineering* (John Wiley & Sons, Inc., Hoboken, NJ, 2016), pp. 1–24.
[14]V. E. Gusev and A. A. Karabutov, *Laser Optoacoustics* (AIP Press, New York, 1993).